

Enhanced Aerosol Mass in the Tropical Tropopause Layer Linked to Ozone Abundance

Shang Liu^{1,*}, Troy D. Thornberry², Pengfei Yu³, Sarah Woods⁴, Karen H. Rosenlof², and Ru-Shan Gao^{2,*}

¹Department of Civil and Environmental Engineering, Northeastern University, Boston, MA 02115, USA

²NOAA Chemical Sciences Laboratory, Boulder, CO, USA

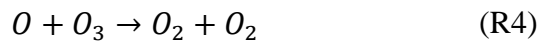
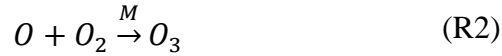
³Institute for Environmental and Climate Research, Jinan University, Guangzhou, China

⁴Earth Observing Laboratory, National Center for Atmospheric Research (NCAR), Boulder, CO

*Correspondence author: shang.liu@northeastern.edu, rushan.gao@noaa.gov

1. Model calculation of ozone profile in the TTL

The natural ozone chemical cycle is described by the Chapman reactions as follows:



The rate equations for [O] and [O₃] are

$$\frac{d[O]}{dt} = 2j_{O_2} - k_2[O][O_2][M] + j_{O_3}[O_3] - k_4[O][O_3] \quad (1)$$

$$\frac{d[O_3]}{dt} = k_2[O][O_2][M] - j_{O_3}[O_3] - k_4[O][O_3] \quad (2)$$

Combining (1) and (2) we obtain

$$\frac{d[O + O_3]}{dt} = 2j_{O_2}[O_2] - 2k_4[O][O_3] \quad (3)$$

Since [O] ≪ [O₃], equation (3) can be written as

$$\frac{d[O_3]}{dt} = 2j_{O_2}[O_2] - 2k_4[O][O_3] \quad (4)$$

30 The fast interconversion between O and O₃ (R2 and R3) leads to the following relationship
 31 between O and O₃ concentrations (Seinfeld and Pandis 2016):

$$\frac{[O]}{[O_3]} = \frac{j_{O_3}}{k_2[O_2][M]} \quad (5)$$

32
 33 Therefore the production rate of O₃ is expressed as

$$\frac{d[O_3]}{dt} = 2j_{O_2}[O_2] - \frac{2k_4j_{O_3}[O_3]^2}{k_2[O_2][M]} \quad (6)$$

34
 35 Where

- 36 • $k_2 = 6.0 \times 10^{-34}(T/300)^{-2.4}$, with an average of $1.7 \times 10^{-33} \text{ cm}^6 \text{ molec}^{-2} \text{ s}^{-1}$ in the TTL.
- 37 • $k_4 = 8.0 \times 10^{-12} \exp(-2060/T)$, with an average of $2.0 \times 10^{-16} \text{ cm}^3 \text{ molec}^{-1} \text{ s}^{-1}$ in the TTL.
- 38 • j_{O_3} ranges from $3 \times 10^{-4} \text{ s}^{-1}$ (SZA=85°) to $6.5 \times 10^{-4} \text{ s}^{-1}$ at SZA = 0° in the TTL (Seinfeld and
 39 Pandis, 2016, Fig. 4.13 on p. 112).
- 40 • j_{O_2} ranges with increasing altitude from $2.0 \times 10^{-15} \text{ s}^{-1}$ to $7 \times 10^{-14} \text{ s}^{-1}$ at SZA = 0° in the TTL
 41 (2016, Fig. 4.12 on p.111).

42
 43 From the observations we have the following average concentrations:

44
 45 $[M] = 1.5 \times 10^{18} \text{ molecules cm}^{-3}$
 46 $[O_2] = 0.21 \times [M] = 3.2 \times 10^{17} \text{ molecules cm}^{-3}$
 47 $[O_3] = 117 \text{ ppb} = 1.9 \times 10^{11} \text{ molecules cm}^{-3}$

48
 49 Using the these values, we find that the first term of equation (6) is $2j_{O_2}[O_2] = 1.2 \times 10^3 - 4.4 \times 10^4$
 50 $\text{molecules cm}^{-3}\text{s}^{-1}$, and the second term of equation (6) is $\frac{2k_4j_{O_3}[O_3]^2}{k_2[O_2][M]} = 5.3 - 11.5 \text{ molecules cm}^{-3}\text{s}^{-1}$,
 51 which can be neglected as it is about 1000 times smaller than the first term. Therefore the O₃
 52 formation rate becomes

53

$$\frac{d[O_3]}{dt} = 2j_{O_2}[O_2] \quad (7)$$

54
 55 We used the vertical profile from Seinfeld and Pandis (2016, Fig. 4.12 on p.111) and the vertical
 56 profile of [O₂] calculated from the measurements to derive the ozone production rate. The
 57 calculated vertical profile of the ozone production rate is shown in Fig. S7. The O₃ concentration
 58 in the TTL is calculated as

59
 60
$$[O_3]_i = [O_3]_{i-1} + \left(\frac{d[O_3]}{dt}\right)_i \cdot \Delta t_i = [O_3]_{i-1} + (2j_{O_2}[O_2])_i \cdot \Delta t_i$$

61
 62 Where i indicates the parameters at altitude i , and Δt_i (5 s) represents the time it takes the air to
 63 rise from altitude $i-1$ to altitude i , using a constant ascent rate of 0.25 mm s^{-1} (Park et al 2010;
 64 Avallone and Prather 1996; Seinfeld and Pandis 2016). The calculation is performed for the

65 altitude range of 14.5–18.9 km, with a prescribed [O₃] at 14.5 km of 28.8 ppb, which represents
66 the average observed O₃ concentration at that altitude.

67

68 **References**

69 Park, S., Atlas, E. L., Jimenez, R., Daube, B. C., Gottlieb, E. W., Nan, J., Jones, D. B. A., Pfister,
70 L., Conway, T. J., Bui, T. P., Gao, R. S. and Wofsy, S. C.: Vertical transport rates and
71 concentrations of OH and Cl radicals in the Tropical Tropopause Layer from observations of CO
72 2 and halocarbons: implications for distributions of long- and short-lived chemical species, *Atmos.*
73 *Chem. Phys.*, 10, 6669–6684, doi:10.5194/acp-10-6669-2010, 2010.

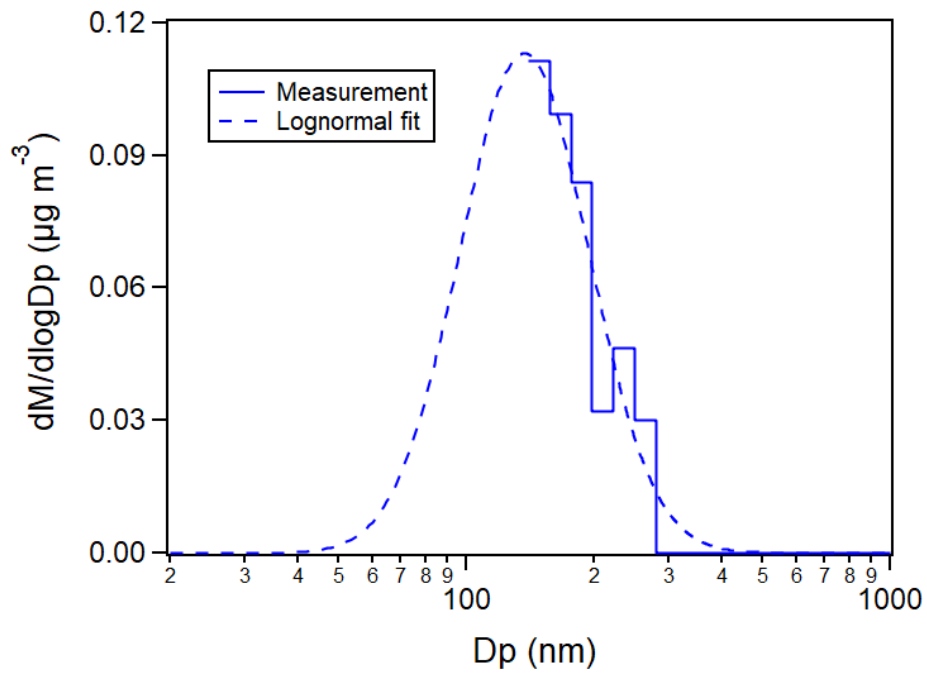
74

75 Seinfeld, J. and Pandis, S.: *Atmospheric chemistry and physics: from air pollution to climate*
76 *change*, Wiley, Hoboken, N. J., 2016.

77 **Supporting Figures**

78

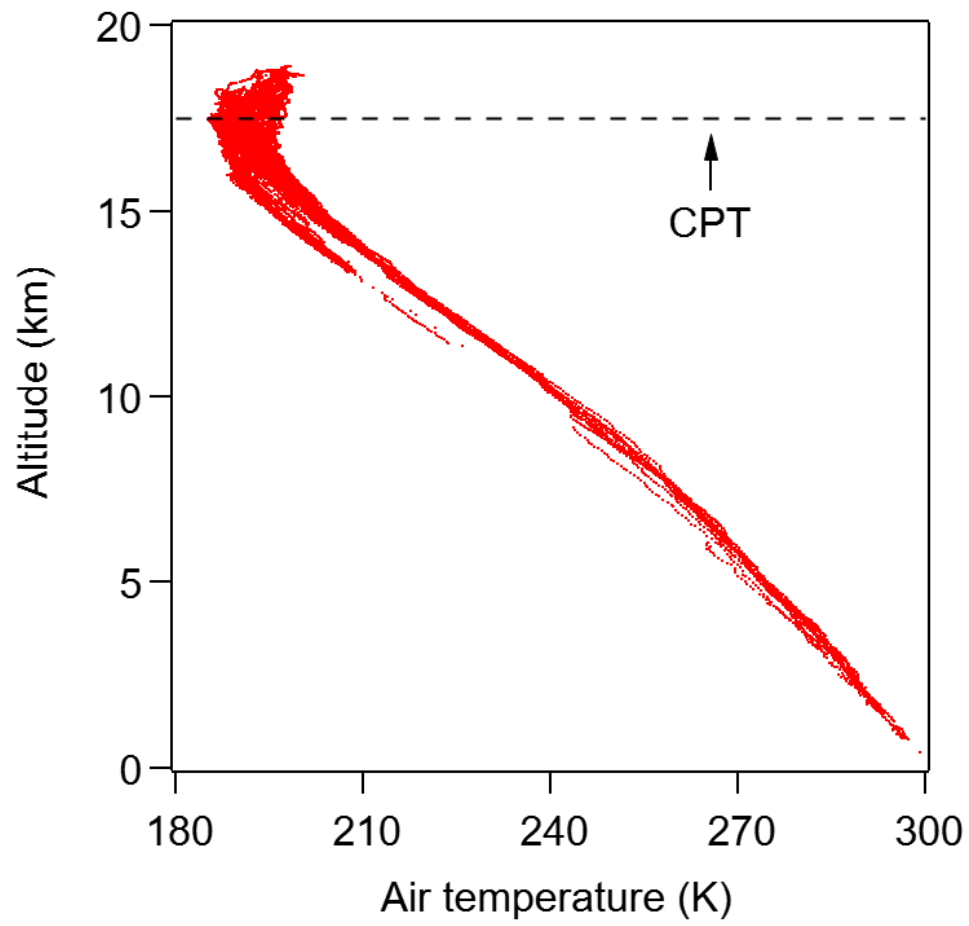
79



80

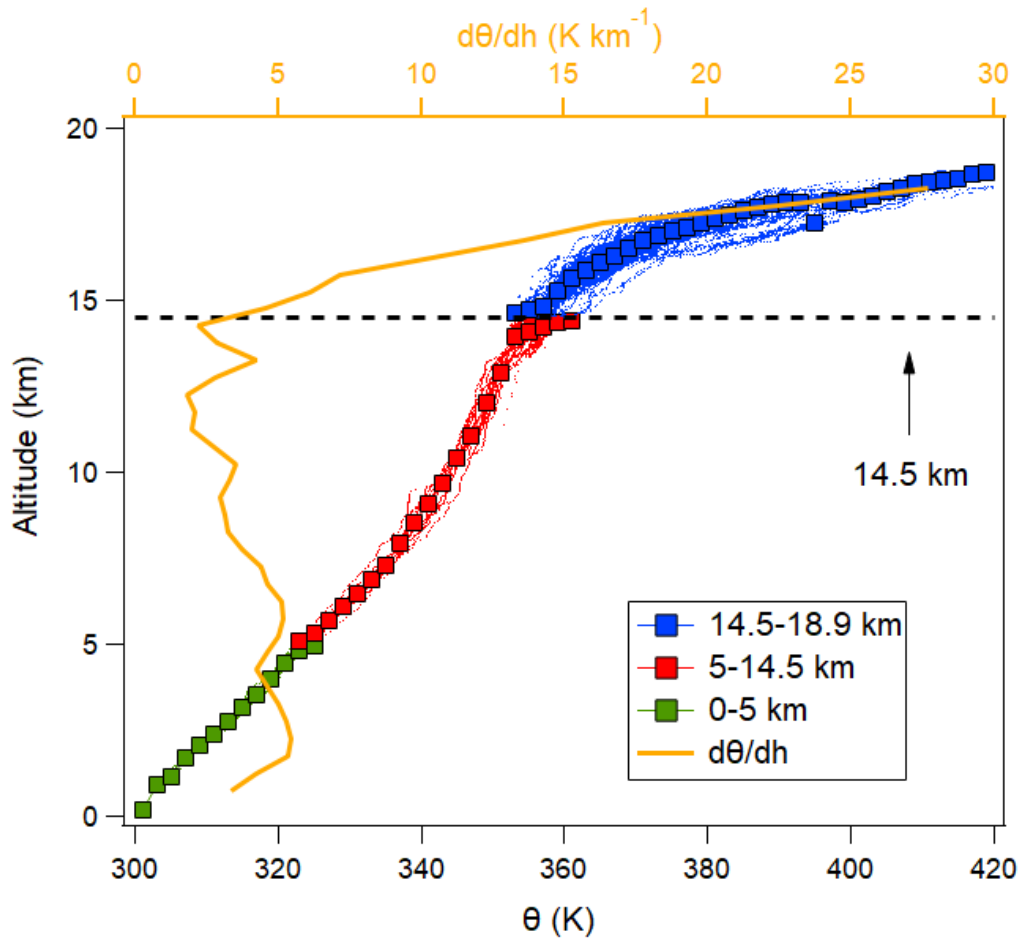
81

82 **Figure S1.** Lognormal fit of the average mass size distribution for the TTL measurements.



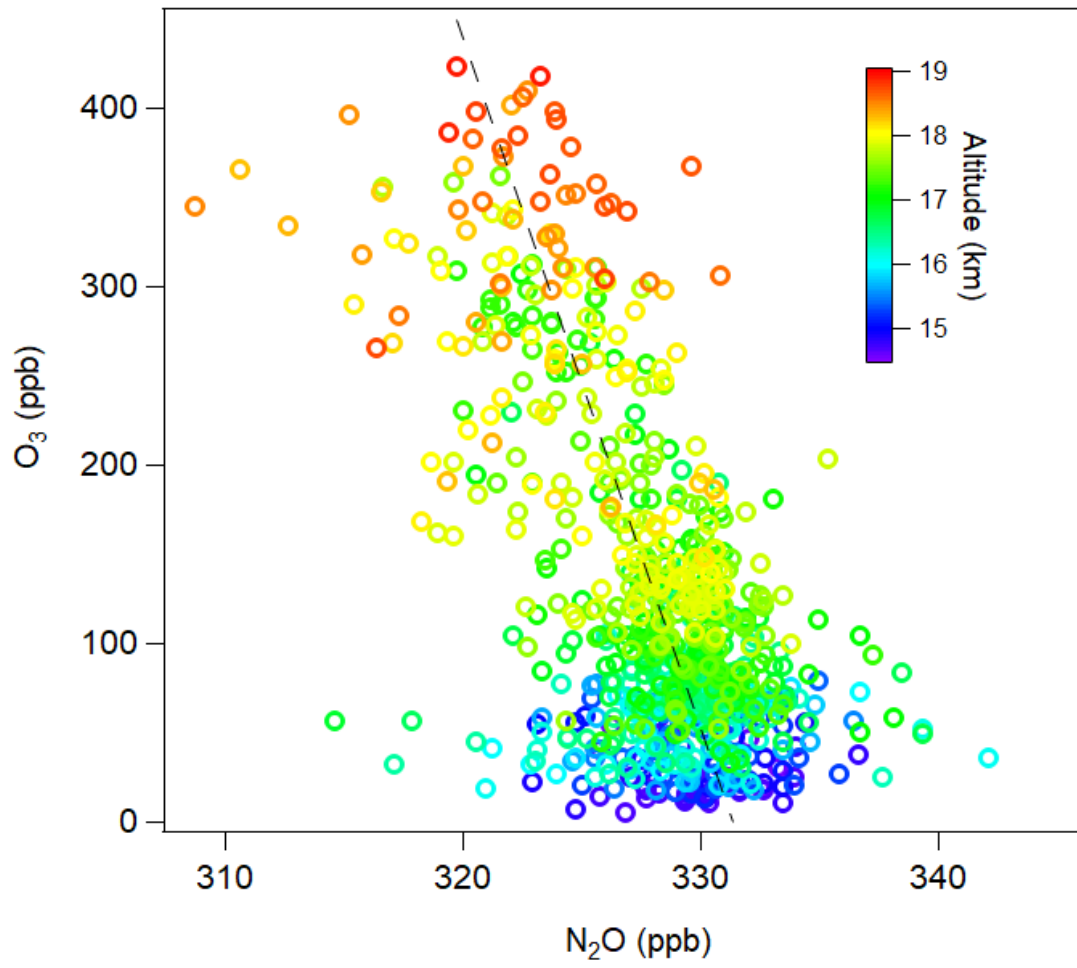
83
84
85

Figure S2. Vertical profile of air temperature measured from all flights.



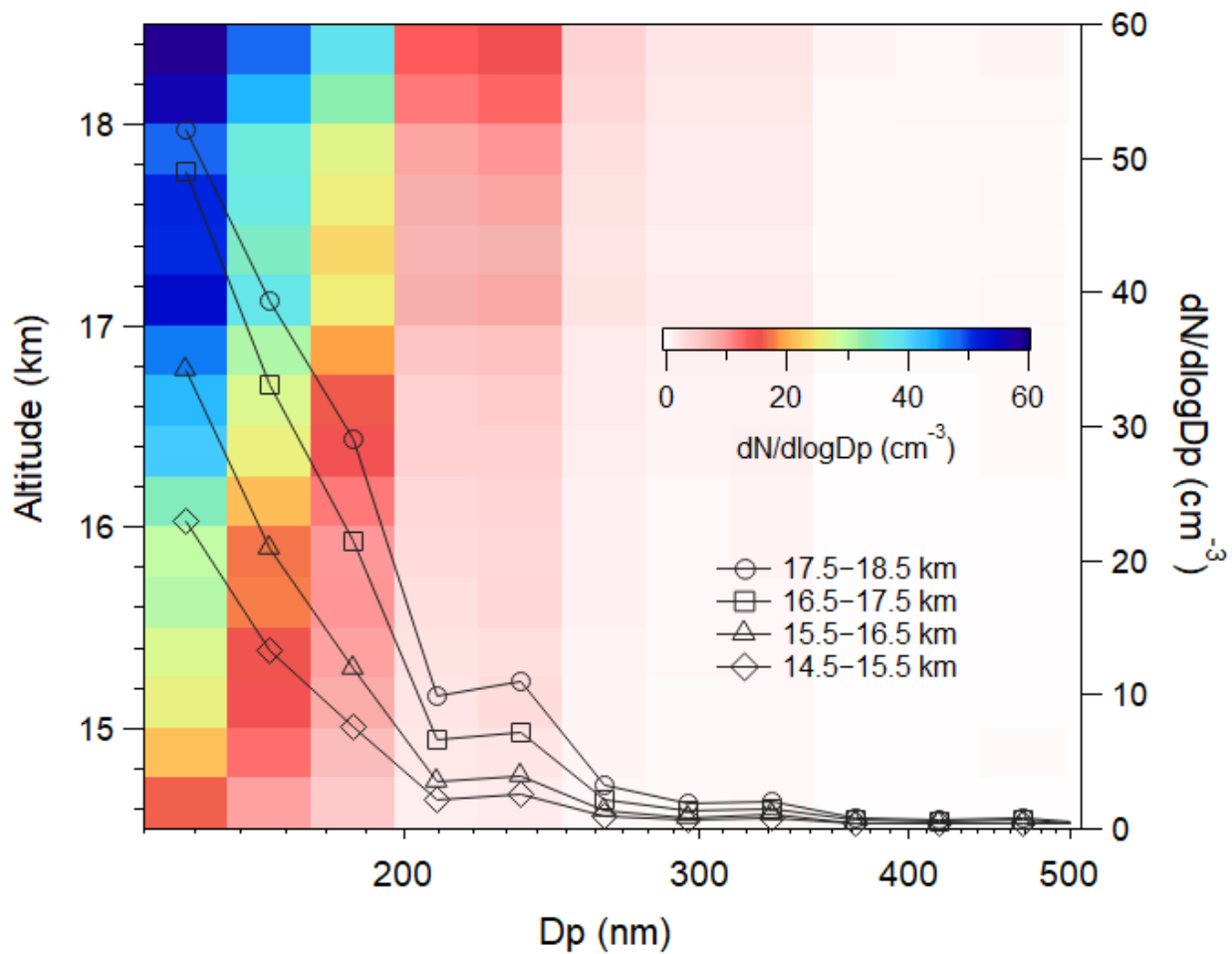
86
 87 **Figure S3.** Vertical profiles of potential temperature (θ) and the lapse rate of θ . In the altitude- θ
 88 profile, individual data points (5-s averages) are shown by the dots and the averages (by θ of 2K)
 89 are shown by the solid squares.

90



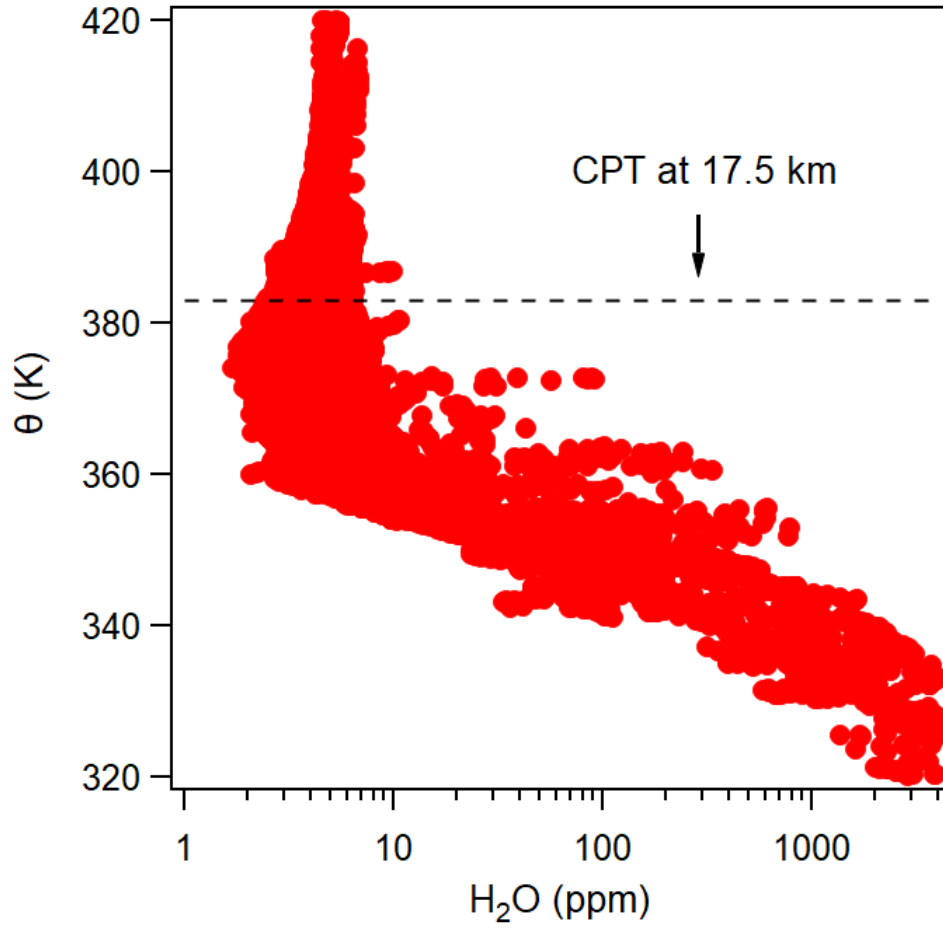
91

92 **Figure S4.** Scatter plot of O₃ versus N₂O in the TTL. The dashed line indicates linear fit.



93
 94
 95
 96
 97

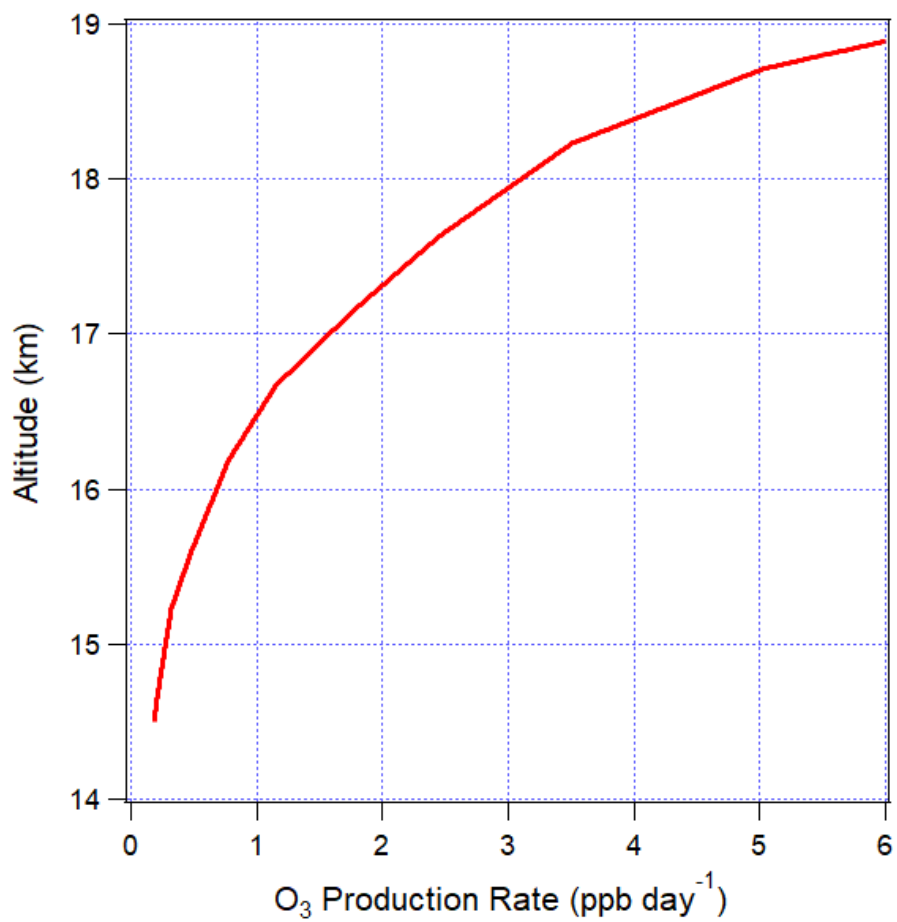
Figure S5. Image plot illustrating aerosol number size distribution with altitude in the TTL. The line and markers represent averages at various altitudinal intervals.



98
99

100 **Figure S6.** θ versus water vapor mixing ratio.

101



102

103

104 **Figure S7.** Calculated vertical profile of ozone production rate in the TTL.